Applied Geomatics (2026) 18:84
https://doi.org/10.1007/s12518-026-00734-x

RESEARCH

Recent (1981–2024) climatic trends in Italy from high-resolution reanalysis data and station-based observations

Alberto Vavassori[1] · **Matej Žgela**[1] · **Maria Antonia Brovelli**[1]

Received: 10 February 2026 / Accepted: 28 April 2026

Abstract
Extreme heat is among the most severe climate-related risks affecting Europe, with particularly pronounced impacts in the Mediterranean region, where temperatures are increasing faster than the global average. In recent decades, the frequency and severity of heatwaves (HWs) have intensified, leading to substantial societal and environmental impacts, including increased heat-related mortality. In this study, we provide a comprehensive assessment of recent climatic trends in Italy over 1981–2024, focusing on daily temperature extremes, HWs, and standard climate and heat stress (HS) indicators. The analysis integrates the VHR-REA_IT climate reanalysis dataset (~ 2.2 km) with ground-based observations from the synoptic network of the Italian Air Force Meteorological Service. Trends are estimated using linear regression and analysed across multiple ecoregions and elevation ranges. Results reveal a clear and spatially coherent warming signal across Italy, characterised by increasing warm extremes, particularly in the frequency of tropical nights (up to +7 days/decade), a marked rise in HW frequency (+2 events/decade), and a widespread reduction in cold extremes. The HS analysis further highlights a growing frequency of thermal discomfort conditions during the warm season, including nighttime periods (up to +8 days/decade), with the strongest increases occurring in lowland and densely populated areas. These findings demonstrate the added value of very high-resolution reanalysis data for tracking spatial patterns in climate trends and provide a valuable basis for stakeholders to support climate adaptation and heat-risk management strategies in Italy under current and future climate change.

Keywords Climatic trends · Heat waves · Heat stress · Climate reanalysis data · Station observations

Introduction

Extreme heat is among the most severe climate-related risks that Europe is expected to face in the near future (European Environment Agency 2024). Over the last 25 years, Europe has experienced the most severe seasons in terms of heat extremes. In particular, a marked increase in the frequency of heat wave (HW) events has been observed since the 1990s (Russo et al. 2015), especially in South-Western Europe (including Spain, France, and Italy), with recent extensions toward Central Europe and Fennoscandia (Boboc et al. 2025). Also, the Mediterranean region has been recognised as a climate change hotspot (Giorgi 2006), where temperatures are projected to rise around 20% faster than the global average (IPCC 2023), partly due to the increasing persistence of subtropical anticyclones (Brunetti et al. 2000).

HW events have severe impacts on ecosystems and society and are associated with increased heat-related mortality during the warm season, particularly among vulnerable groups such as children and the elderly. For instance, during the summer 2022 HW, more than 60,000 heat-related fatalities were estimated across Europe, with the highest absolute number and mortality rate reported in Italy (Ballester et al. 2023).

In this context, warm and cold temperature extremes represent key indicators for assessing climate trends and patterns. At the regional and national scale, the analysis of extreme temperature trends provides valuable information for stakeholders, supporting the design and implementation of climate adaptation strategies (Fioravanti et al. 2016). To enable standardised assessments and facilitate comparisons

✉ Alberto Vavassori
alberto.vavassori@polimi.it

[1] Department of Civil and Environmental Engineering, Politecnico di Milano, Piazza Leonardo da Vinci 32, Milano 20133, Italy

Published online: 12 May 2026

across regions, significant efforts have been devoted to developing synthetic climatic indicators. In particular, the standard indices proposed by ETCCDI (Expert Team on Climate Change Detection and Indices) (Zwiers and Zhang 2009) have been adopted worldwide, including in Europe (Domínguez-Castro et al. 2020), the Mediterranean (Turco et al. 2013), North America (Terando et al. 2012), and Central Asia (Sajjad and Ghaffar 2019). In addition to indices based on maximum and minimum daily temperatures, heat stress (HS) indicators are widely used to assess the thermal discomfort experienced by the population during extreme heat episodes (Yasmeen and Liu 2019; Rachid and Qureshi 2023). In fact, although a relation has been found between high air temperature and excess mortality during an HW event (Campbell et al. 2018), HS indices are more appropriate to describe the impact of extreme heat on human health, which depends on a combination of meteorological factors, including e.g., air temperature, relative humidity, and wind speed (Mora et al. 2017).

The analysis of climate trends is typically conducted using long-term station-based observations, which provide direct measurements. Examples can be found both at the continental (Klein Tank and Können 2003; Simolo et al. 2014) and national (Fioravanti et al. 2016; Settanta et al. 2024) scales. Alternatively, climate reanalysis products are exploited when spatially continuous information on climatic trends is sought; these datasets have been used in both global (Simmons et al. 2017) and regional studies, e.g. in Europe (Peña-Angulo et al. 2020; Croce et al. 2021; Bilgili and Tokmakci 2025). Many studies rely on reanalysis data with relatively coarse spatial resolution, such as ERA5 (31 km) and ERA5-Land (9 km), albeit with the advantage of long temporal coverage. More recently, high-resolution national reanalyses have been developed in multiple countries, such as Germany (1 km) (Krähenmann et al. 2018) and Italy (2.2 km) (Raffa et al. 2021), with recent efforts also aimed at providing near-real-time reanalysis products (Manco et al. 2025).

In the present study, the focus is on Italy, where the assessment of extreme heat events and climate trends is particularly relevant given that the country is among the 10 oldest populations worldwide (United Nations, 2024) and the oldest population within the European Union (Eurostat 2025). Several studies have investigated climate variability and extremes at the national scale, including analyses of temperature trends for 1961–2004 (Toreti and Desiato 2008); temperature, precipitation, and extreme events over the last century (Brunetti et al. 2004); and daily temperature extremes for 1865–1996 (Brunetti et al. 2000), also using standard indices (Fioravanti et al. 2016). Recently, a comprehensive analysis of summer heat extremes and HWs for the period 1991–2020 was conducted, focusing on HW frequency, intensity, and duration (Settanta et al. 2024). Regional-scale analyses have also been performed for specific regions, e.g. Trentino-Alto Adige (Morlot et al. 2023), Tuscany (Bartolini et al. 2012), Calabria (Prete et al. 2023), and Abruzzo (Scorzini and Leopardi 2019; Curci et al. 2021).

Despite the wealth of studies focusing on the Italian context, some gaps remain. In particular, to the best of our knowledge, no previous study has investigated recent climatic trends over Italy, integrating high-resolution reanalysis data with station observations. Existing studies are primarily based on station measurements, while reanalysis products have been mostly employed for regional-scale assessments (e.g. the Mediterranean region), often using coarser spatial resolutions. Furthermore, previous work has generally focused either on HW characteristics or on climate indices, while a joint assessment of daily temperature extremes, HWs, and HS conditions is still lacking. To address these gaps, the objectives of this work are:

- to investigate recent (1981–2024) trends in temperature extremes in Italy, with particular focus on daily maximum and minimum temperatures, HWs, and selected ETCCDI indices, by combining a very-high resolution climate reanalysis dataset with ground-based observations from an authoritative synoptic network;
- to assess trends in thermal discomfort conditions at different times of the day through an HS index;
- to explore the differences in trends across multiple geographical regions and elevation ranges.

The remainder of this paper is organised as follows. Section 2 describes the study area and the employed dataset. Section 3 presents the methodology. The results are outlined in Sect. 4 and discussed in Sect. 5. Finally, the main conclusions are drawn in Sect. 6.

Data

Study area

The study focuses on Italy, which extends across the central Mediterranean basin, approximately between 36°N and 47°N in latitude and 6°E and 19°E in longitude. Owing to its large geographical extent, complex topography, and proximity to the Mediterranean Sea, Italy exhibits a wealth of diverse climatic conditions (Fratianni and Acquaotta 2017).

According to the widely adopted Köppen-Geiger classification system (Kottek et al. 2006), most of the Po Plain and Adriatic coast fall within a humid subtropical climate (Cfa), while Liguria, the Tyrrhenian coast, and most of southern

Italy, including Sicily and Sardinia, are characterised by a hot-summer Mediterranean climate (Csa), transitioning to warm-summer Mediterranean (Csb) conditions at higher elevations. Oceanic climates (Cfb) prevail near the Alpine foothills and along the Apennines, with a further transition to humid continental (Dfb) and alpine tundra (ET) climates at the highest altitudes.

To analyse recent climatic trends across Italy, we adopted the subdivision of the territory into ecoregions proposed by Blasi et al. (2014). This classification delineates homogeneous areas from an ecological perspective, combining basic data on climate, geomorphology, vegetation, and land cover. In this study, ecoregions were selected as the basic spatial units of analysis because they combine climatic characteristics with land-system properties, providing a more suitable framework than administrative boundaries or purely climatic classifications for interpreting climate signals and supporting land management and adaptation strategies.

The ecoregion system includes seven Provinces: Alpine (1A), Po Plain (1B), Apennine (1C), Illyrian (1D), Ligurian-Provencal (2A), Tyrrhenian (2B), and Adriatic (2C). Due to their limited spatial extent, Provinces 1D and 2A were merged with the neighbouring Po Plain (1B) and Tyrrhenian (2B) Provinces, respectively, so that each spatial unit is represented by a meaningful number of ground-based meteorological stations and an adequate sample of pixels from the climate reanalysis product, as described in the following Sections. As a result, the study area was divided into five ecoregions. The original classification is described in detail in Blasi et al. (2014), and the ecoregion boundaries are shown in Fig. 1.

Climate reanalysis data

Ground-based observations are commonly used to assess temporal trends of climate indices. However, their spatial coverage is limited, leaving large areas insufficiently

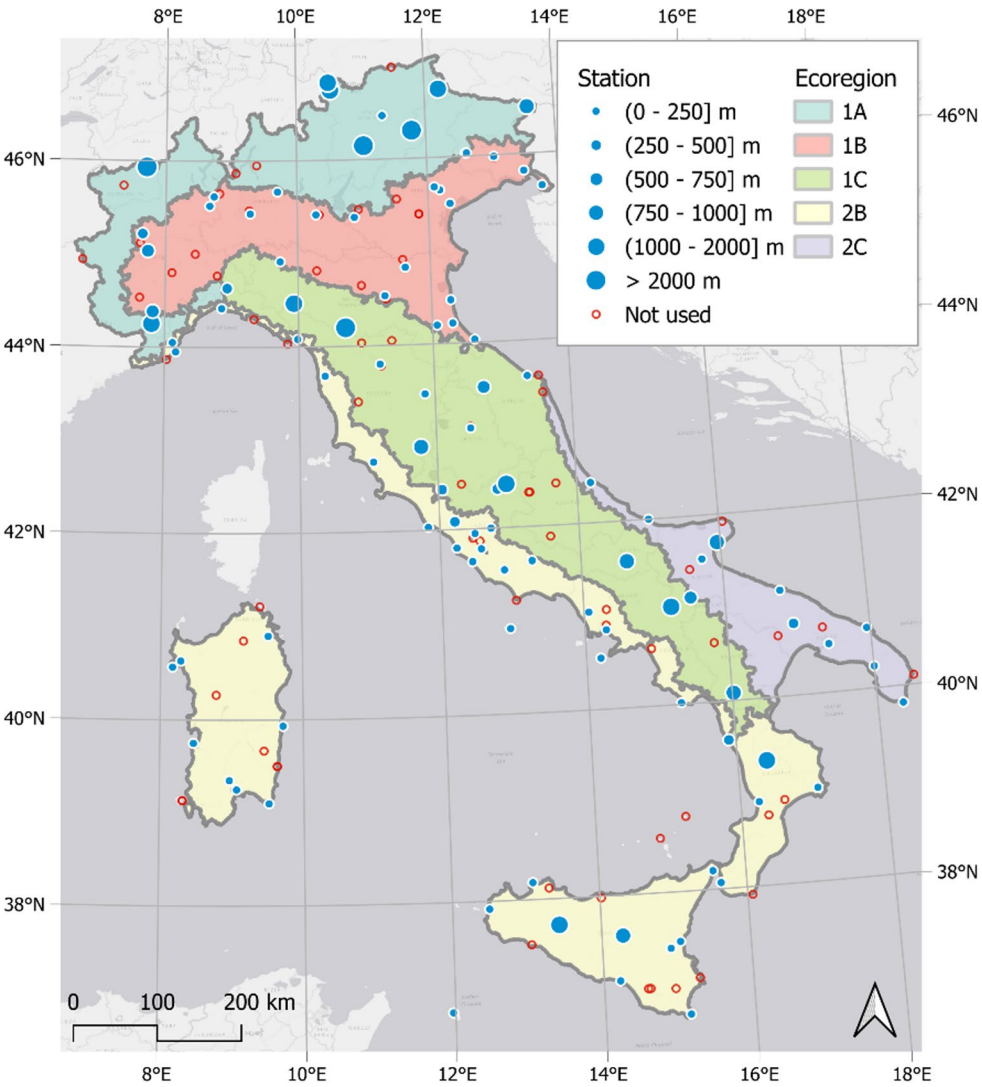

Fig. 1 Location of the ground-based stations and subdivision of Italy into ecoregions (1A: Alpine; 1B: Po Plain; 1C: Apennine; 2B: Tyrrhenian; 2C: Adriatic). The size of the dots is proportional to the site elevation. Red-outlined dots indicate stations with time series completeness less than 70%, which have not been used for the analysis. Basemap: Esri Gray (light) © Esri

represented. Gridded long-term reanalysis data, therefore, offer a clear advantage when spatial patterns of climatic trends are of interest. To analyse recent climatic trends, we relied on a high-resolution climate reanalysis dataset that provides spatially continuous coverage across the Italian peninsula.

We exploited the VHR-REA_IT (Very High-Resolution dynamical downscaling of ERA5 Reanalysis over Italy) dataset, developed by the Euro-Mediterranean Centre on Climate Change (Centro Euro-Mediterraneo sui Cambiamenti Climatici, CMCC) (Raffa et al. 2021; Adinolfi et al. 2023). VHR-REA_IT was developed by dynamically downscaling the ERA5 reanalysis over Italy (Hersbach et al. 2020), originally at ∼ 31 km, using the COSMO-CLM regional climate model (Rockel et al. 2008).

VHR-REA_IT provides a detailed and comprehensive representation of meteorological conditions over Italy, both in terms of spatial and temporal resolutions, making it suitable for investigating climatic trends. In particular, it provides hourly data of multiple meteorological variables at ∼ 2.2 km resolution, currently covering the period 1981–2024. This high spatial resolution enables the detection of fine-scale thermal features, such as temperature differences within complex orography and urban heat islands.

However, as a downscaled product, VHR-REA_IT suffers from some known biases that are both seasonal and elevation-dependent when evaluated against gridded observational datasets. As shown by Cavalleri et al. (2024), a warm bias of up to 3 °C can be expected over flat terrains during summer, particularly in northern Italy. In winter, the product exhibits a cold bias which increases toward higher elevations. Despite these biases, VHR-REA_IT remains a valuable high-resolution dataset for analysing spatial climate patterns at the regional scale.

VHR-REA_IT was retrieved using the dedicated Python library *ddsapi* (https://pypi.org/project/ddsapi/, last accessed on 22 January 2026), which enables direct and efficient access to CMCC's Data Delivery System API. Daily maximum (T_{max}) and minimum (T_{min}) air temperatures were downloaded for the analysis of trends in climate indices. In addition, daily dew point temperature (T_d) and hourly air temperatures at selected times, as described in Sect. 3.4, were retrieved for the analysis of HS trends.

Ground-based station data

In situ observations of air temperature, collected by ground-based meteorological stations, were also exploited. These data were retrieved from the Italian national system for the collection, elaboration and diffusion of climatological data (SCIA, Sistema Nazionale per l'Elaborazione e Diffusione di Dati Climatici), which gathers data from multiple sources, including synoptic networks and different meteorological, hydrological, and agrometeorological networks (Desiato et al. 2011; https://scia.isprambiente.it/, last accessed on 25 January 2026).

This system provides multiple quality-controlled climate statistics and indicators at different time resolutions, as well as several climatic products. The first set of quality controls is applied by each data provider to detect erroneous raw values. Additionally, data are controlled every year through a set of systematic routines derived from those implemented for the GHCN (Global Historical Climatological Network) before being made available in the SCIA database, in order to filter out invalid or erroneous data (Durre et al. 2010).

For the purposes of the present work, the stations belonging to the synoptic network of the Italian Air Force Meteorological Service were considered, as they provide authoritative data compliant with the World Meteorological Organisation (WMO) standards (WMO 2024) and they feature a satisfactory time series completeness compared to the stations belonging to the other networks. Accordingly, the daily T_{max} and T_{min} temperature records for the period 1981–2024 were downloaded from the SCIA database. The spatial distribution of the stations is depicted in Fig. 1, while the time series availability for both maximum and minimum daily temperatures is provided in the supplementary material.

Methods

In this Section, the methodology adopted for the data processing and analysis is presented. An overview of the methodological flow is provided in Fig. 2.

Pre-processing of the station data

For the purposes of analysing the long-term climatic trends, the availability of continuous and complete time series is a key requirement. For this reason, stations were first filtered according to the completeness of both daily T_{max} and T_{min} records. In particular, all stations with a completeness lower than 70% were excluded from the subsequent analysis. This threshold was chosen as a suitable trade-off between ensuring sufficiently complete time series and retaining a large number of stations in the analysis. The same criterion was adopted in previous work on HW trend analysis in Italy (Settanta et al. 2024). As a result, out of the initial 178 stations belonging to the synoptic network, 100 (56%) and 103 (58%) stations satisfied the completeness requirements for T_{max} and T_{min} records, respectively, and were therefore retained for the following quality-control procedure.

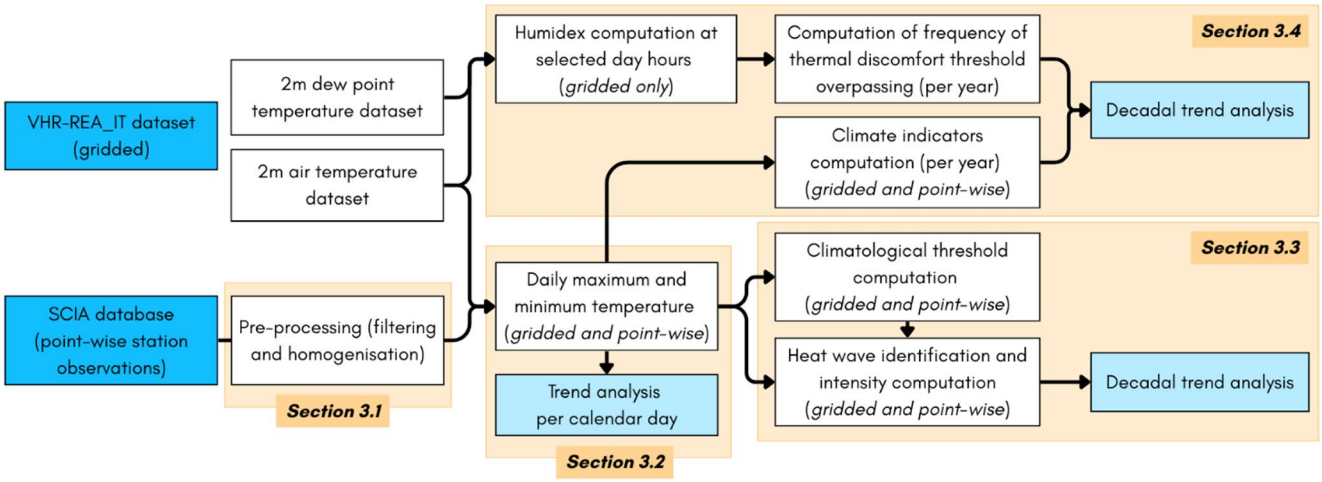

Fig. 2 Flowchart summarising the methodological workflow

As a second step, the homogeneity of the time series was assessed to account for artificial and non-climatic factors (e.g., changes in instrumentation, station relocation, or land-use modifications) that may negatively affect the estimate of climate trends. In principle, station metadata can provide valuable information to detect artificial discontinuities (breakpoints) in the time series (Peterson et al. 1998); however, when metadata are unavailable or insufficiently detailed, the homogeneity assessment is typically performed using statistical methods (Toreti and Desiato 2008; Fioravanti et al. 2016; Fratianni and Acquaotta 2017). In this work, owing to the lack of detailed information on the station locations and surrounding conditions, the homogeneity of temperature time series was evaluated using the Climatol procedure, as implemented in the R package *climatol* (version 4.3.0) (Guijarro 2018), following previous work (Settanta et al. 2024).

Climatol assesses the homogeneity of each time series by applying the Standard Normal Homogenization Test (SNHT, Barriopedro et al. 2023) to the anomaly series computed between observed data and a reference time series. The reference series is derived from the neighbouring stations, selected based on geographical proximity using Euclidean distances. However, when the station distribution is sparse, the reference series may originate from a different climatic region, which can negatively affect the homogenisation performance. To mitigate this problem, the homogenisation procedure was applied separately to each group of stations within each ecoregion.

As recommended by Guijarro (2018), the daily temperature records were first aggregated to monthly means, and time series breakpoints were identified on the resulting monthly time series. Eventually, each daily time series was adjusted using the corresponding monthly breakpoints. Furthermore, the Climatol tool was exploited to fill gaps in the station records. To minimise the uncertainties associated with the time series interpolation, only gaps of one or two consecutive days were filled using interpolated values, while longer gaps were left unfilled.

Trends of daily maximum and minimum temperature per calendar day

A first analysis was carried out to assess the temporal trends of T_{max} and T_{min} for each calendar day across the different ecoregions, with the aim of identifying periods of the year that experienced higher or lower warming rates over the past 44 years (1981–2024). Temperature trends were evaluated independently for both the pixels of the VHR-REA_IT dataset and the ground-based stations and analysed separately for each ecoregion.

To achieve this result, the median daily temperature time series was computed by aggregating all pixels (and, separately, all stations) belonging to each ecoregion, for both T_{max} and T_{min} records. The resulting median time series was then smoothed using a centred rolling average with a $\pm$15-day window. Starting from the original (median) time series, this procedure provided a new time series in which each value represents the average conditions over a 31-day window centred on the corresponding calendar day. Note that, to ensure consistency across the years and properly handle leap years, observations recorded on February 29th were removed by averaging them with the corresponding values of February 28th; in this way, we obtained 365 time series, each consisting of 44 values.

For each calendar day, the long-term temperature trend was then estimated by fitting a linear regression to the 44 annual values of T_{max} or T_{min} corresponding to that day. The slope of the regression line provided an estimate of the temperature trend. In this study, the statistical significance

of the trend is indicated by a p-value less than 0.05, unless otherwise specified. Accordingly, the resulting time series of regression slopes represents the magnitude of long-term temperature trends for each calendar day, allowing us to infer the warming (or cooling) rate throughout the year.

Identification and trend analysis of HW events

In addition to the analysis of the warming rates over the year based on daily T_{max} and T_{min}, trends in HW events were also investigated. Several methods have been proposed in the literature to identify HWs, as no universally accepted definition exists (Barriopedro et al. 2023). Depending on the study objective and the region under investigation, different criteria may be adopted, typically involving a minimum duration and a minimum intensity, defined in terms of threshold exceedance. In this study, the approach proposed by Perkins and Alexander (2013) was followed.

Accordingly, an HW was defined as a period of at least three consecutive days during which T_{max} exceeds the 90th percentile of long-term (1981–2024) daily T_{max} for the corresponding calendar day. The threshold was computed after applying a centred ± 15-day moving average to the daily T_{max} time series, in order to smooth the day-to-day variability. Note that the computation of the climatological threshold had to be performed for each calendar day and for each pixel of the VHR-REA_IT dataset, as well as for each station, which implied a remarkable computational burden. For this reason, this step was carried out using Google Colab.

For each reanalysis pixel and for each station, all HW events were identified, and, for every year, the total number of HW events was computed along with the average HW duration and intensity. HW intensity is defined as the excess heat, that is, the difference between the daily T_{max} and the corresponding long-term climatological threshold, averaged over the event duration. Ultimately, trends in the total number of annual HW events and in average HW duration and intensity were quantified as the slope of a linear regression fitted to the corresponding annual time series.

Trend analysis of climate indicators and HS

To complement the analysis of warming rates and HW trends described in the previous Sections, we investigated the spatial patterns and temporal trends of selected ETCCDI indices based on daily T_{max} and T_{min}. In particular, the following indices were selected and computed for each year:

- summer days index: number of days with $T_{max} > 25$ °C,
- hot days index: number of days with $T_{max} > 30$ °C,
- very hot days index: number of days with $T_{max} > 35$ °C,
- tropical nights index: number of days with $T_{min} > 20$ °C,
- frost days index: number of days with $T_{min} < 0$ °C,
- ice days index: number of days with $T_{max} < 0$ °C.

These indices were calculated both for each grid cell of the VHR-REA_IT dataset and for each ground-based station.

A further analysis was performed to explicitly account for HS conditions, which are more directly related to human thermal comfort and health impacts. For this purpose, the Humidex HS index was computed as a proxy of the perceived HS (Schwingshackl et al. 2021). Humidex is defined as a function of near-surface air temperature and dew point temperature and was thus only computed using the VHR-REA_IT dataset for each grid pixel, due to the unavailability of the latter variable data for the ground-based stations.

The HS analysis was restricted to the warm half of the year (April-September), and for selected hours of the day, namely 2 AM, 7 AM, 2 PM, and 8 PM, representative of nighttime, early morning, afternoon, and evening conditions, respectively, when the population's exposure to thermal discomfort is most relevant. For each grid cell and time of day, the frequency of Humidex threshold exceedances was computed yearly, following the thresholds defined in (Government of Canada 2025). Specifically, a Humidex threshold of 30 (corresponding to "some" thermal discomfort) was adopted for all hours except 2 PM, for which a threshold of 40 (indicating "great" thermal discomfort) was used.

Consistent with the trend analyses described in the previous Sections, the trends in all indices (both climatic and HS indices) were estimated using linear regression, with the slope of the regression line representing the magnitude of the linear trend. Furthermore, the differences in the trends among the different ecoregions and elevation ranges were investigated. Indeed, elevation modulates temperature regimes, and trend magnitudes may therefore differ substantially between lowland and mountainous areas. For this purpose, eight elevation ranges were defined, namely 0–50 m, 50–100 m, 100–200 m, 200–500 m, 500–1000 m, 1000–1500 m, 1500–2000 m, and over 2000 m.

Results

Trends of daily maximum and minimum temperatures

The decadal trends in daily T_{max} and T_{min} over the period 1981–2024 reveal a clear and spatially coherent warming across all ecoregions (see Fig. 3). The variability of the temporal trends across the VHR-REA_IT grid pixels

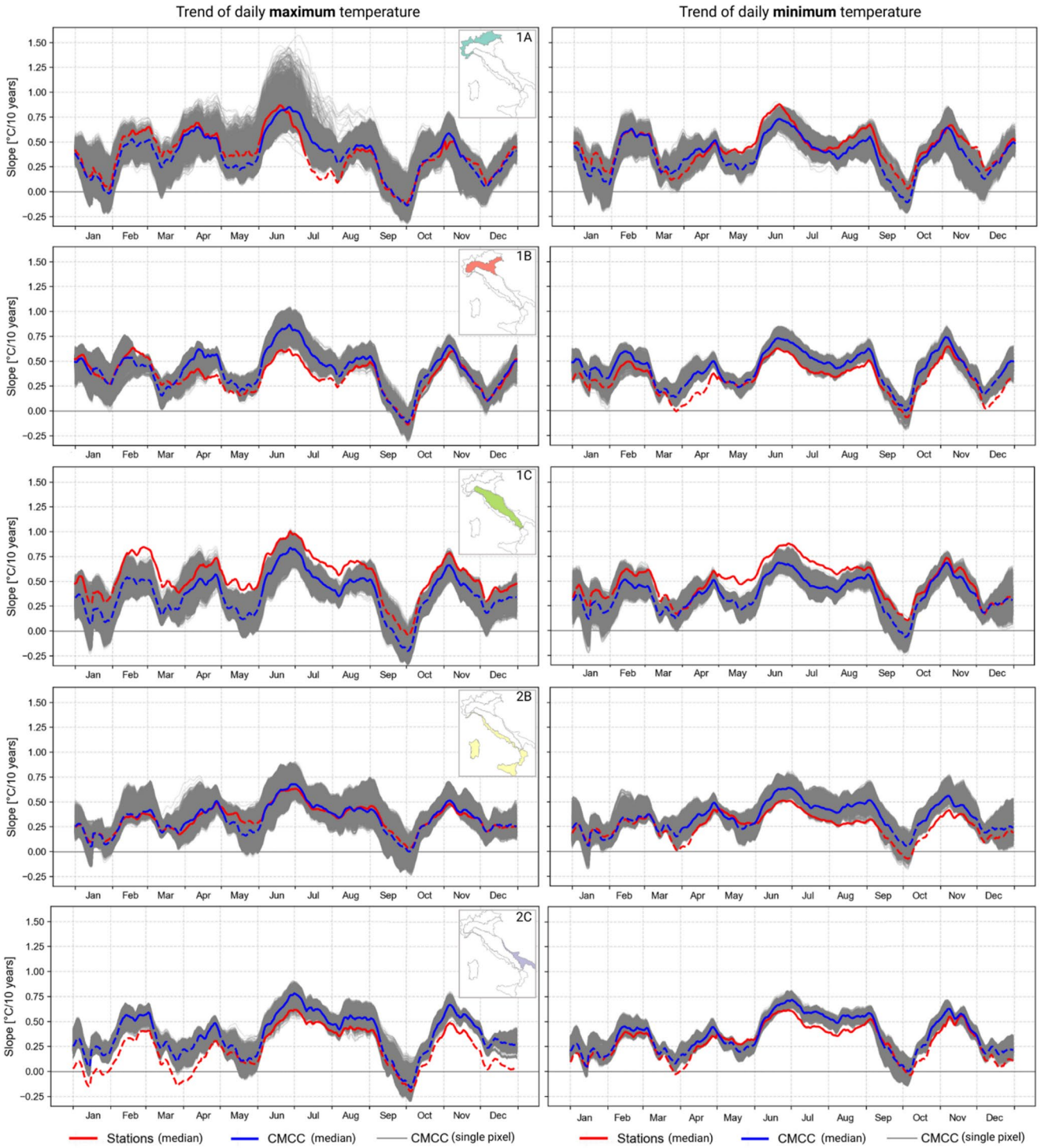

Fig. 3 Temporal trend of daily maximum and minimum temperatures across the ecoregions. Temperature series were smoothed using a ± 15-day rolling average, and the median time series was computed, separately, for all pixels of the CMCC dataset and the station observations. Dashed lines indicate statistically non-significant results (p-value > 0.05)

is more pronounced for T_{max}, particularly for the Alpine region (ecoregion 1A), while more homogeneous trends are observed for T_{min} within each ecoregion.

A comparison between the trends estimated from the reanalysis dataset and those derived from ground-based station observations shows an overall agreement in both magnitude and temporal evolution. This agreement is especially evident for the Alpine (1A) and Tyrrhenian (2B) ecoregions, for both T_{max} and T_{min}. In contrast, station observations indicate a systematically stronger warming trend for the Apennine region (1C), and a slightly lower warming rate in the Po Plain (1B) and Adriatic (2C) regions. Nevertheless, differences between the two datasets remain limited and are always below 0.25 °C/decade. It is worthwhile highlighting that the largest differences between the two datasets mostly occur in cases where one of the two trends is statistically non-significant, such as the T_{max} trend from the reanalysis in ecoregion 1C and the station-based T_{max} trend in ecoregion 2C.

A marked intra-annual variability in the decadal warming rate is found, with the most pronounced warming occurring during summer, particularly in June, when rates reach up to 1 °C/decade. For some pixels of the reanalysis dataset in Alpine (1A) ecoregion, peak values exceed 1.25 °C/decade during this month, suggesting that the most relevant increases in T_{max} affect the mountainous areas. Significant warming is also observed in winter, between December and January and during February, especially in the Po Plain (1B) and Apennine (1C) regions. In contrast, little or no evident warming is detected between the second half of September and early October, as well as between late November and early December, when trends are close to zero across all ecoregions; relatively weaker warming rates are also observed in May.

Finally, a comparison of the temporal evolution of trends among the different ecoregions highlights that the Tyrrhenian (2B) and Southern Adriatic (2C) regions generally exhibit slightly lower warming rates (usually less than 0.75 °C/decade) and reduced intra-annual variability compared to the other regions.

Trends of HW events

The number of HW events shows a clear increase over time, as illustrated in Fig. 4. This upward trend is spatially consistent across the study area, with average rates ranging from 1.4 events/decade in ecoregion 1A to 1.7 events/decade in ecoregion 1B, as estimated from the reanalysis. Intermediate average values are found in ecoregion 2C (1.5 events/decade) and in ecoregions 1C and 2B (1.6 events/decade). Median values closely match the corresponding means, indicating that the distributions are not substantially affected by outliers. Although the increase in HW days is widespread, some spatial heterogeneity can be identified. The strongest trends are found in the Po Plain (1B) and the Tyrrhenian region (2B), with particularly

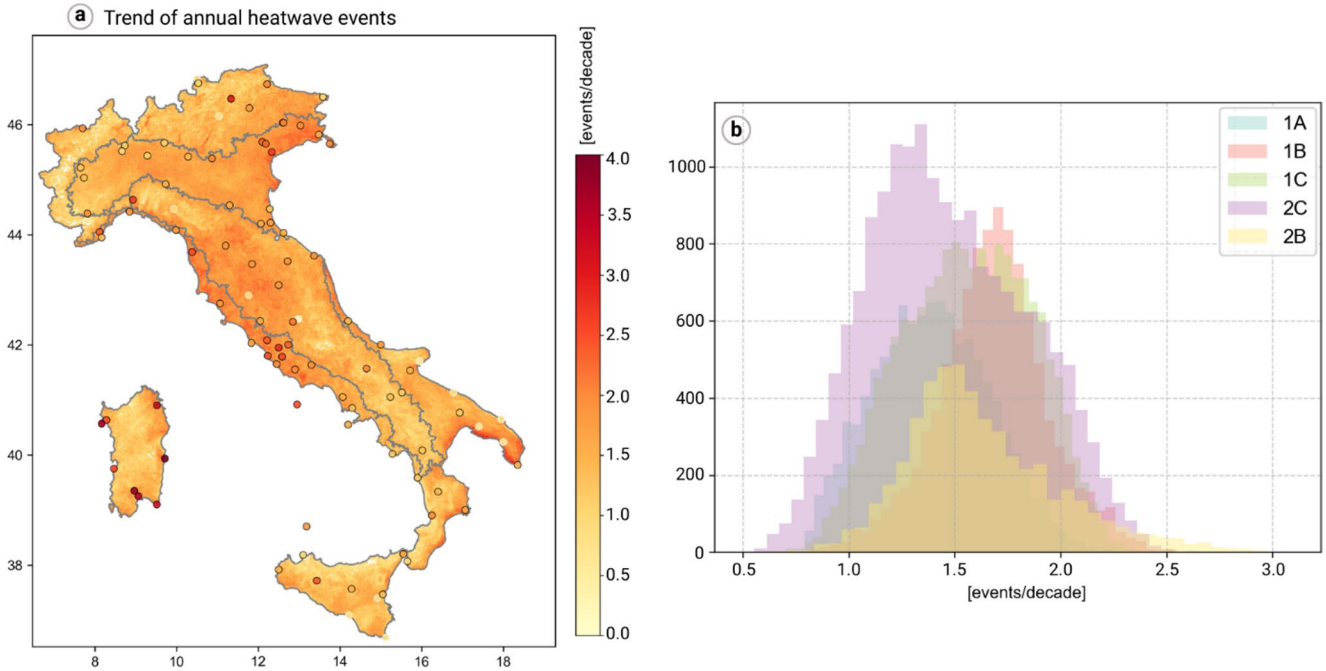

Fig. 4 (**a**) Trend in the number of HW events estimated from the VHR-REA_IT dataset (per grid pixel) and from station observations; (**b**) histogram of trend values per ecoregion from the VHR-REA_IT dataset. For VHR-REA_IT, white pixels indicate statistically non-significant trends (p-value > 0.05). For station observations, statistically significant trends (p-value < 0.05) are indicated by black-outlined symbols

high rates in the north-eastern Po Plain and along the central Tyrrhenian coast, in agreement with trends derived from station observations. In addition, the Ionian sector of Puglia exhibits high rates as well. Conversely, relatively weaker trends are observed in the Alpine region and, more generally, in southern Italy, including Sicily. A comparison between trends obtained from the VHR-REA_IT dataset and those derived from station observations shows overall good agreement, with a mean absolute difference of 0.5 events/decade. Considering the spatial distribution of the differences, only a few regional discrepancies can be identified. In particular, station-based estimates indicate slightly higher trends over Sardinia.

About HW duration and intensity, only weak positive trends are detected, on the order of 0.25 days/decade and 0.1 °C/decade, respectively. However, the majority of pixels and stations do not exhibit statistically significant trends for this metric; therefore, these results are not discussed further in this Section.

For the sake of completeness, the average number of HW events, HW days, and the corresponding average duration and intensity in each ecoregion are reported in the Appendix.

Climate indicators and HS trends

In this Section, the results of the analysis of climatic indicators and HS metrics are presented. The spatial patterns of trends in the selected climate indicators, along with their corresponding distribution by ecoregion, are represented in Figs. 5 and 6.

A first noteworthy result is the good agreement between trends computed from the VHR-REA_IT dataset and those obtained from station observations, supporting the overall robustness and reliability of the results. The agreement is observed both in terms of trend magnitude and statistical significance. For indices based on daily T_{max}, absolute mean differences between the two datasets amount to 1.7 days/decade for warm days and 2.0 days/decade for both hot and very hot days; a slightly lower absolute difference is found for ice days, equal to 1.5 days/decade. For the indices based on daily T_{min}, absolute mean differences equal 2.4 days/decade for tropical nights and 2.3 days/decade for frost days.

Focusing on summer, hot, and very hot day indicators (Fig. 5), positive trends are detected over most of the study area. Exceptions are limited to the highest mountainous regions, where T_{max} thresholds are rarely exceeded,

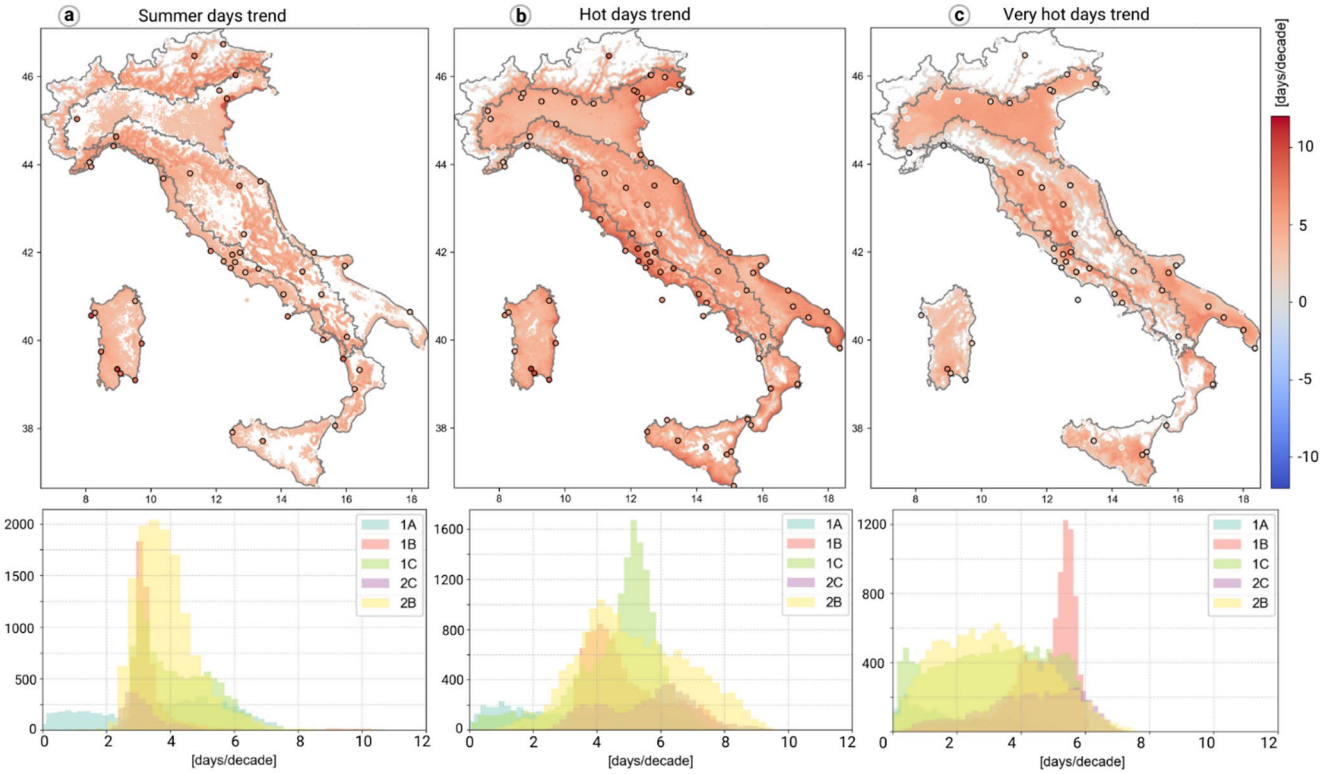

Fig. 5 Spatial distribution of trends in the annual number of (**a**) summer days ($T_{max} > 25$ °C), (**b**) hot days ($T_{max} > 30$ °C), and (**c**) very hot days ($T_{max} > 35$ °C), together with the corresponding trend distributions for each ecoregion. For VHR-REA_IT, white pixels indicate statistically non-significant trends (p-value > 0.05). For station observations, statistically significant trends (p-value < 0.05) are indicated by black-outlined symbols

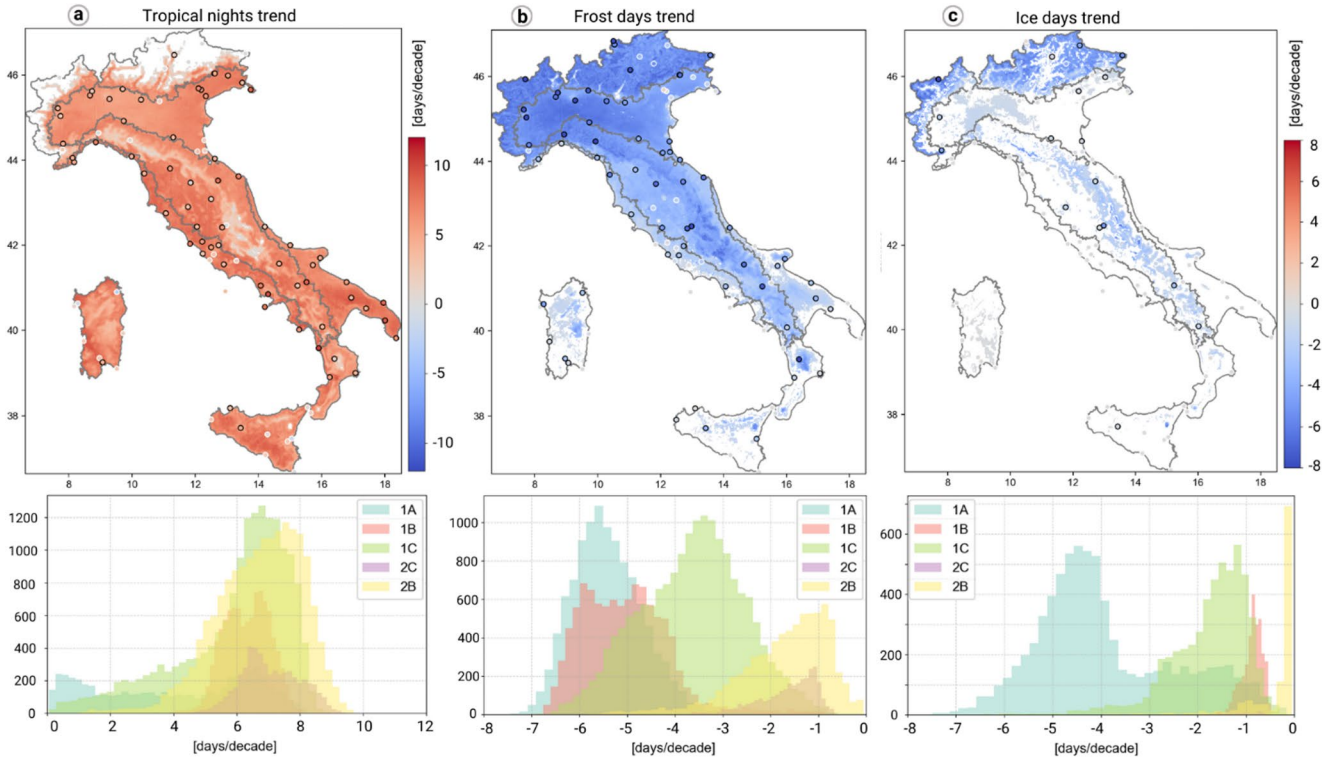

Fig. 6 Spatial distribution of trends in the annual number of (**a**) tropical nights ($T_{min} > 20$ °C), (**b**) frost days ($T_{min} < 0$ °C), and (**c**) ice days ($T_{max} < 0$ °C), together with the corresponding trend distributions for each ecoregion. For VHR-REA_IT, white pixels indicate statistically non-significant trends (p-value > 0.05). For station observations, statistically significant trends (p-value < 0.05) are indicated by black-outlined symbols. Distinct colour ramp ranges are applied for frost days and ice days

and trends are therefore statistically non-significant (and anyway close to zero). For summer days ($T_{max} > 25$ °C), trends are relatively homogeneous across all ecoregions, with mean values ranging from ~ 3.5 (ecoregion 1B) to 4.1 (ecoregion 1C) days/decade. While trends in lowland areas are spatially consistent, higher rates are observed in foothill and lower-elevation mountainous regions, such as along the Apennines, indicating that the 25 °C threshold is being exceeded at progressively higher altitudes.

Trends in hot days ($T_{max} > 30$ °C) are more pronounced than those for summer days and show a consistent spatial pattern across lowland areas, with average values ranging from 4.8 days/decade in ecoregion 1B to 5.6 days/decade in ecoregion 2C. The highest rates are found in coastal areas, especially along the central Tyrrhenian coast. In contrast, trends in very hot days ($T_{max} > 35$ °C) are strongest over inland low-altitude areas, with the largest mean increase observed in the Po Plain (4.7 days/decade). However, it should be noted that the trends of very hot days estimated across the Po Plain from the reanalysis are higher than those obtained with the station observations, which, in turn, are mostly statistically non-significant. This result can be explained by the known warm bias of the VHR-REA_IT dataset during the summer season across the lowlands.

Among all temperature-based indicators, tropical nights exhibit the largest increase over time (Fig. 6), with the highest average trends in ecoregions 2C (7.0 days/decade), 2B (6.7 days/decade), and 1B (6.3 days/decade), and peak values close to 10 days/decade.

Conversely, frost and ice days display widespread negative trends (Fig. 6), confirming the persistence of warming also during the cold season. In particular, the decrease in the annual number of frost days ($T_{min} < 0$ °C) is largest in the Alpine (1A) and Po Plain (1B) regions, with mean values equal to −5.4 and −5.0 days/decade, respectively. In the lowlands, the most pronounced decrease is found for the Po Plain, indicating progressively rarer winter days when T_{min} goes below 0 °C. A similar but weaker decrease is observed in the Apennine region (1C) (−3.6 days/decade), whereas lower rates characterise the remaining regions due to the lower frequency of frost-day occurrence. For the same reason, for ice days ($T_{max} < 0$ °C), statistically significant trends are mainly detected in the Alpine and Apennine regions, and to a lesser extent in the Po Plain, with mean decreases of −3.9 days/decade in the Alps and −1.8 days/decade in the Apennines. Anyway, it is important to highlight that statistically non-significant trends correspond to values close to zero.

The considerations outlined above regarding the different patterns in lowland and mountainous areas are further supported by the analysis of trends across different elevation ranges, depicted in Figs. 7 and 8. For summer days (Fig. 7), the largest average trends are found between 500 and 1000 m (4.4 days/decade) and 1000–1500 m (4.3 days/decade), while slightly lower values occur at lower elevations (3.5–3.8 days/decade).

In contrast, hot and very hot days, as well as tropical nights, exhibit relatively uniform increases at elevations below 500 m, with high rates also extending into the 500–1000 m range for hot days and tropical nights. For very hot days, trends decrease sharply above this elevation, confirming that the 35 °C threshold is rarely exceeded above 1000 m. These patterns are consistently observed in both the reanalysis and station datasets, with statistically significant trends primarily found at lower elevations. For elevations below 1000 m, average trends derived from VHR-REA_IT range from 4.3 to 5.6 days/decade for hot days and from 1.9 to 4.5 days/decade for very hot days, while tropical nights display the strongest increases, particularly in the 200–500 m elevation class (7.0 days/decade).

The strongest dependence on elevation is observed for frost and ice days, whose decreasing trends get larger as altitude increases. In particular, a remarkable decrease in ice days is found above 1000 m, with average values between −3.4 days/decade (1000–1500 m) and −5.1 days/decade above 2000 m. While the station trends are generally coherent with the reanalysis estimates, the Pian Rosa station (3500 m a.s.l.) exhibits very remarkable and statistically significant rates, ∼ −17 days/decade in both frost and ice days.

Finally, HS conditions were assessed through the analysis of Humidex threshold exceedances at different times of the day (Figs. 9 and 10). While we comment only on the trends in the threshold exceedances, the actual yearly average numbers of exceedances in each ecoregion are reported in the Appendix. Overall, HS trends are strongly dependent on elevation, with the lowest positive rates observed in the ecoregions 1A and 1C. Across all hours, trends decrease systematically with increasing elevation, remaining relatively uniform up to 500 m, beyond which a marked reduction is observed.

Among ecoregions, the strongest positive trends are generally found in the Adriatic (2C) and Tyrrhenian (2B) regions, followed by the Po Plain (1B), with similar spatial patterns at all hours. For the Humidex threshold of 30 (indicating "some" thermal discomfort), the highest increases occur during the evening (8 PM) and early morning (7 AM), when average trends in ecoregion 2C reach 7.4 and 7.7 days/decade, respectively. Comparable values are observed in ecoregions 2B and 1B. Lower trends are found at 2 PM, when a threshold of 40 ("great" thermal discomfort) is considered; nevertheless, average increases still range between 2.3 days/decade (ecoregion 2B) and 3.3 days/decade (ecoregion 1B).

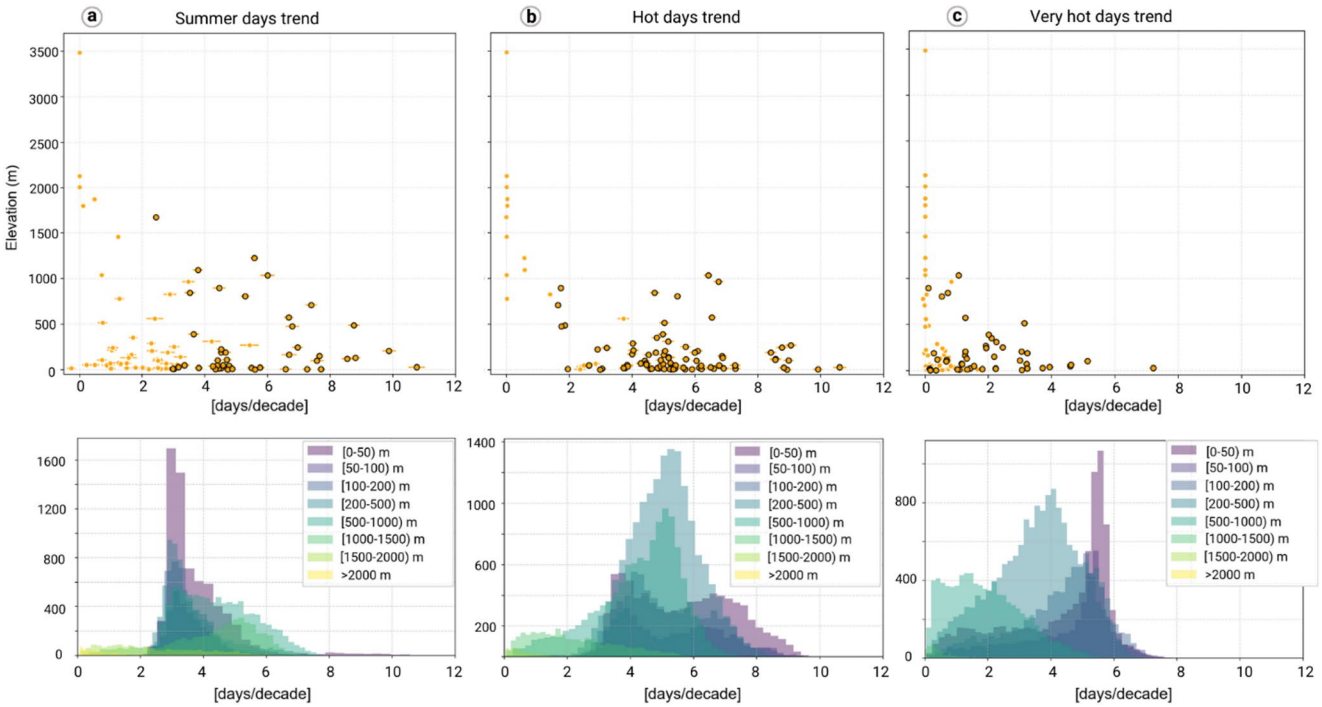

Fig. 7 Trend of (**a**) summer days, (**b**) hot days, and (**c**) very hot days per elevation range. Upper panels: trends obtained from station observations (statistically significant trends are indicated by black-outlined symbols). Lower panels: histograms of trends obtained from the VHR-REA_IT dataset

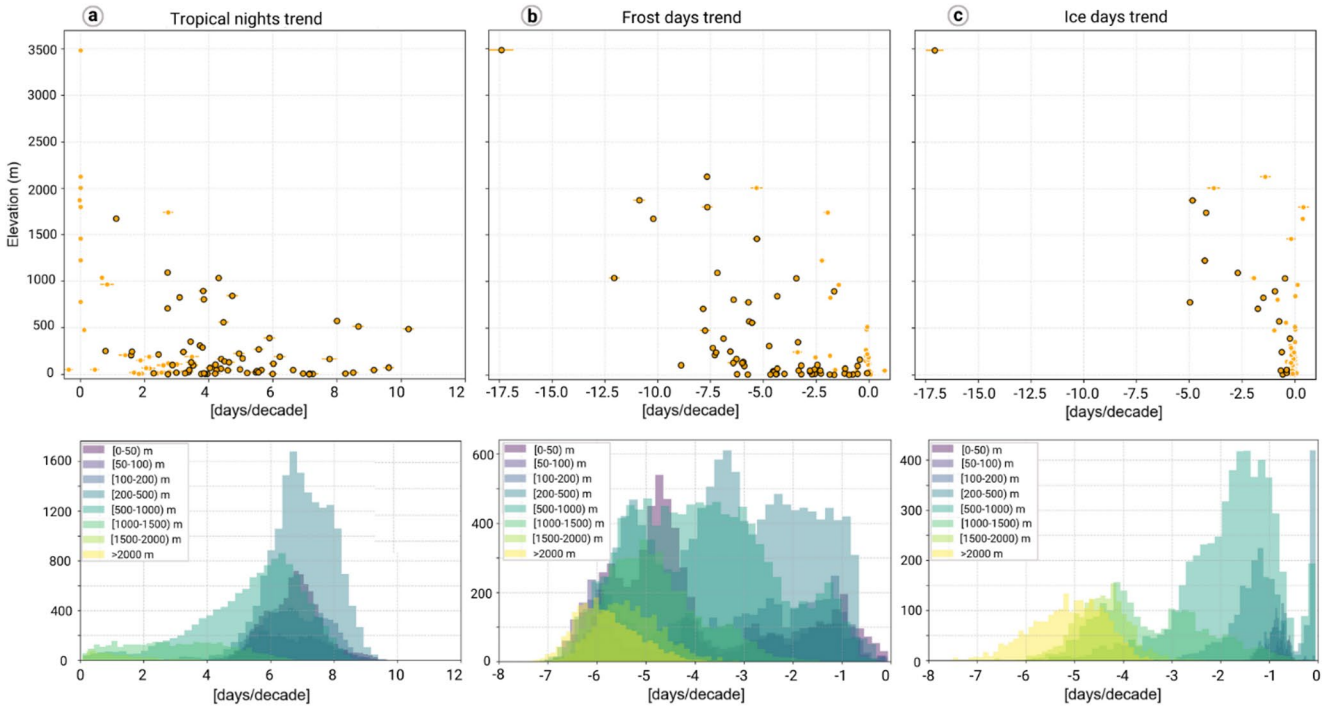

Fig. 8 Trend of (**a**) tropical nights, (**b**) frost days, and (**c**) ice days per elevation range. Upper panels: trends obtained from station observations (statistically significant trends are indicated by black-outlined symbols). Lower panels: histograms of trends obtained from the VHR-REA_IT dataset

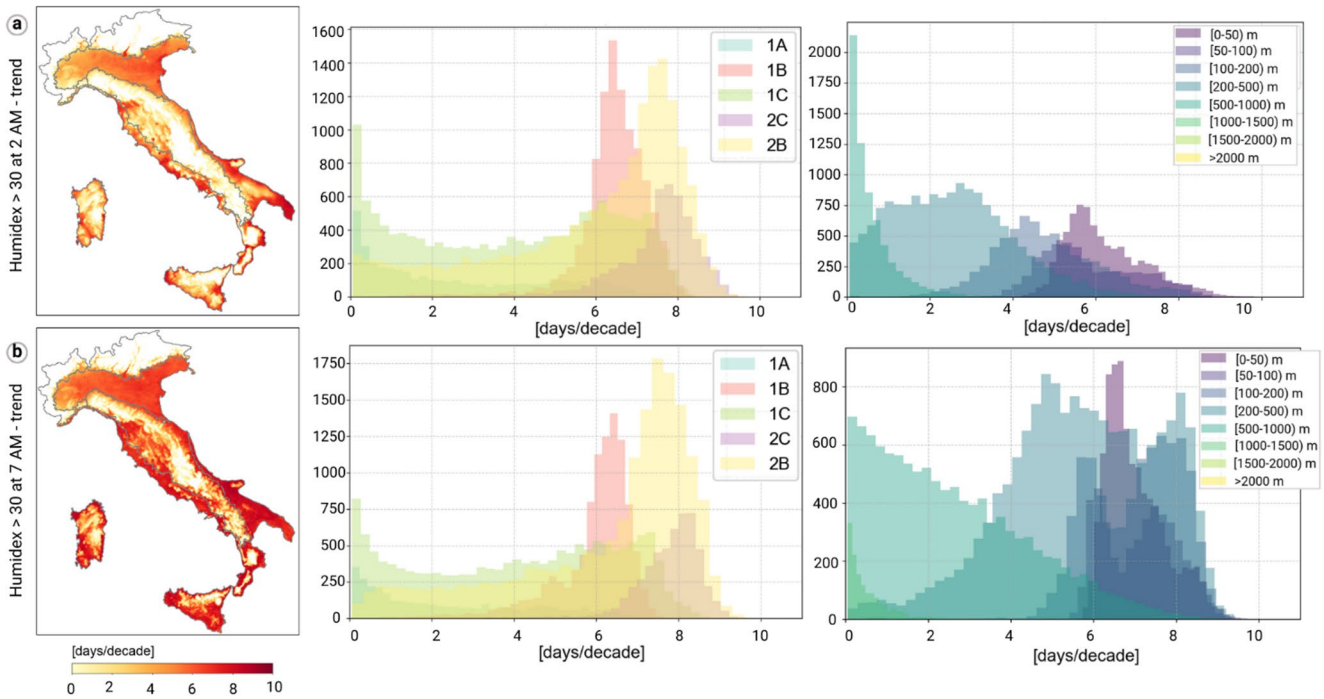

Fig. 9 Trends in the number of annual occurrences of (**a**) Humidex > 30 at 2 AM and (**b**) Humidex > 30 at 7 AM. The spatial distribution of the decadal trend [days/decade] is shown along with the corresponding histogram distributions per ecoregion and elevation range. White pixels indicate statistically non-significant trends (p-value > 0.05)

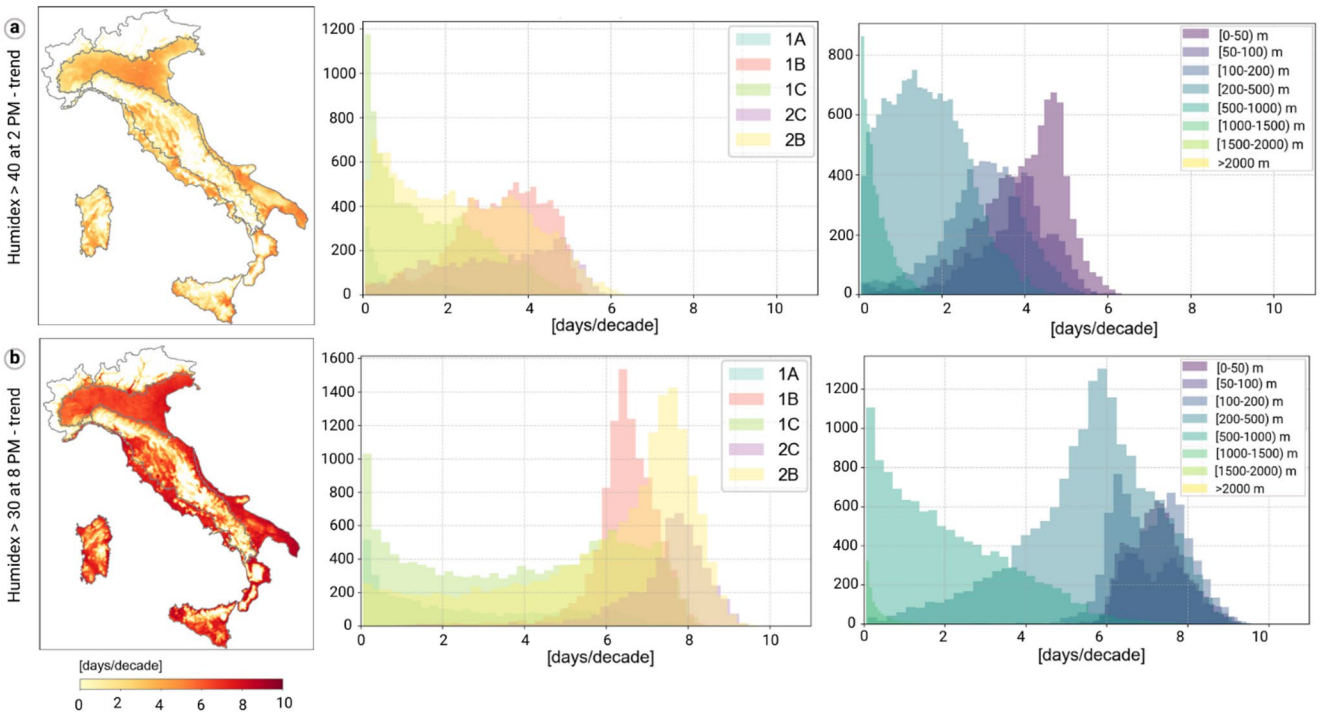

Fig. 10 Trends in the number of annual occurrences of (**a**) Humidex > 40 at 2 PM and (**b**) Humidex > 30 at 8 PM. The spatial distribution of the decadal trend [days/decade] is shown along with the corresponding histogram distributions per ecoregion and elevation range. White pixels indicate statistically non-significant trends (p-value > 0.05)

Discussion

The warming trends detected over 1981–2024 are consistent with earlier studies, which identified a shift from cooling to sustained warming in Italy beginning around the late 1970s. Toreti and Desiato (2008) and Fratianni and Acquaotta (2017) both reported increasing T_{max} and T_{min} after 1980, with rates of about 0.5 to 0.6 °C/decade for T_{max} and 0.4 to 0.5 °C/decade for T_{min}, in close agreement with values observed in this study across most ecoregions. The stronger summer warming identified here, with peak rates approaching or exceeding 1 °C/decade in June, confirms previous findings that warming in Italy and the Mediterranean is most pronounced during summer months (Kostopoulou and Jones 2005; Brunet et al. 2007; Donat et al. 2013). The somewhat higher warming observed in the Alpine and Apennine regions is also consistent with earlier evidence of enhanced warming at high elevations.

HW frequency has increased across Italy, in line with broader European and Mediterranean trends (Perkins-Kirkpatrick and Lewis 2020; IPCC 2023; Boboc et al. 2025). By analysing HWs at high spatial resolution and on an annual basis, this study shows that the increase is strongest during 2011–2024, indicating a recent acceleration in HW occurrence that is not always captured in shorter or seasonally restricted analyses. In contrast, HW duration does not show a clear long-term increase and typically remains between 4 and 6 days, differing from studies that report HW lengthening in other Mediterranean regions (Galanaki et al. 2022; Díaz-Poso et al. 2023). While this study focuses on the annual HW frequency, seasonal analysis confirms that HW days increase most strongly in summer, consistent with previous findings for Italy (Settanta et al. 2024). Changes in HW intensity are weak (around +0.1 °C/decade) and mostly non-significant, contrasting with studies reporting intensification, likely due to differences in metrics and study periods. Overall, recent warming in Italy appears to manifest primarily through more frequent HWs and a growing number of HW days, rather than longer or more intense events.

Warm-related indicators show widespread and largely statistically significant increases, while cold-related indicators exhibit consistent and often significant declines, particularly in mountainous regions. High-elevation areas show strong sensitivity to warming, with temperature thresholds being exceeded at progressively higher altitudes, confirming the well-known vulnerability of mountainous and Alpine regions to climate change (Kohler and Maselli 2009; Gobiet et al. 2014). The detected trends are consistent with those reported by Fioravanti et al. (2016), who analysed station-based data across Italy and found marked decreases in frost days (−4.2 days/decade) and increases in summer days and tropical nights (+4.7 days/decade) during 1978–2011. In the present study, tropical nights increase even more rapidly, reaching about +6 to 7 days/decade, suggesting that

nighttime warming has intensified further in recent years. This behaviour is in line with previous evidence that recent warming is generally more pronounced for indices based on T_{min} (Donat et al. 2013).

Dangerous heat conditions, expressed through Humidex exceedance, are increasing most in coastal areas and flat regions, where much of the population lives. Although few studies provide spatially explicit HS trend analysis, our results closely match HS hotspots identified using the Thermal Pressure Index by Yavaşlı (2025), particularly in the Po Valley, Tyrrhenian coast, Puglia, and Sicily. The main driver of HS trends is the steady rise in T_{max}, which directly increases the Humidex, together with the influence of humidity. Scoccimarro et al. (2017) showed that future Humidex increases across Europe are linked to rising air specific humidity, whose role warrants further investigation. In Italy, coastal areas experience higher moisture due to sea evaporation, while the Po Valley often has weak air circulation, allowing warm and moist air to accumulate and intensify HS. Despite stronger trends near the coast, thermal discomfort may be partly reduced by sea-breeze cooling (Sirangelo et al. 2020), an effect absent inland. With projected increases in temperature and associated humidity changes (Lee et al. 2021), population exposure to extreme heat is expected to rise, increasing the need for reliable, spatially explicit HS knowledge. In this context, the national-scale assessment presented here provides a climatic basis that supports applied studies linking HS to health outcomes, such as those reported by Infusino et al. (2021).

Some limitations of this study should also be acknowledged. Reanalysis datasets are known to exhibit biases, particularly in representing temperature extremes, although the overall trends show good agreement with station observations. Some differences between the two sources may be related to the uneven spatial distribution of ground stations and to incomplete station time series. In addition, trends were estimated using linear regression, which does not account for potential non-linear behaviour or changes in warming rates over time. Finally, HS was assessed using the Humidex index alone, and further work is required to provide a comprehensive estimate.

Conclusions

In this paper, a comprehensive assessment of climatic trends over the last 44 years (1981–2024) in Italy was presented. This analysis is especially relevant in view of the recent rise in extreme heat across Europe, which has strongly affected the Mediterranean region and Italy.

The study exploited the VHR-REA_IT very high-resolution climate reanalysis dataset (2.2 km resolution) covering the whole Italian territory, along with ground-based station observations from the synoptic network of the Italian Air Force Meteorological Service. The integration of these kinds of data allowed us to evaluate the consistency and reliability of the reanalysis-based results, demonstrating the added value of very high-resolution climate reanalysis products for national-scale analyses, particularly in countries characterised by complex orography (such as Italy). Indeed, it was possible to underscore differences across narrow elevation ranges that would be hard to detect using coarser-resolution datasets.

We investigated daily temperature extremes throughout the year, including a set of ETCCDI indices based on maximum and minimum temperatures, as well as HW events and HS conditions. Their trends were quantified using linear regression and explored across multiple ecoregions and elevation ranges, in order to track spatial differences in the magnitude and pattern of warming (or cooling). To the best of our knowledge, no previous study has provided such a comprehensive evaluation of recent climate trends in Italy by integrating ground-based station observations and very-high resolution climate reanalysis data.

Results reveal a clear and spatially coherent warming across Italy, consistent among ecoregions and elevation classes, with only slightly lower rates observed in the southern regions. Overall, these changes indicate a shift toward more frequent warm extremes and fewer cold events. Key findings can be outlined as follows:

- a warming trend in daily maximum and minimum temperatures is observed throughout the year, with the strongest increase occurring in summer, reaching rates up to 1.0 °C/decade; similarly, an increase in the frequency of HW events is recorded, on the order of ∼ 2 events/decade;
- among all climate indices, tropical nights exhibit the largest and most widespread increase (∼ 6 days/decade, on average), followed by hot days (∼ 5 days/decade, on average), except at the highest elevations; a remarkable increase in the frequency of thermal discomfort conditions during the warm season is also recorded, both in the afternoon hours and nighttime, in agreement with the more frequent tropical nights; although trends are strongly modulated by elevation, the largest rise occurs in lowland areas, implying that a large fraction of the population is increasingly exposed to adverse HS conditions.

The outcomes of this study are statistically robust and provide a solid scientific basis for supporting climate adaptation strategies, heat risk preparedness, and public health planning, particularly with regard to protecting the most vulnerable population groups from increasing extreme heat risks under the ongoing climate change.

Appendix

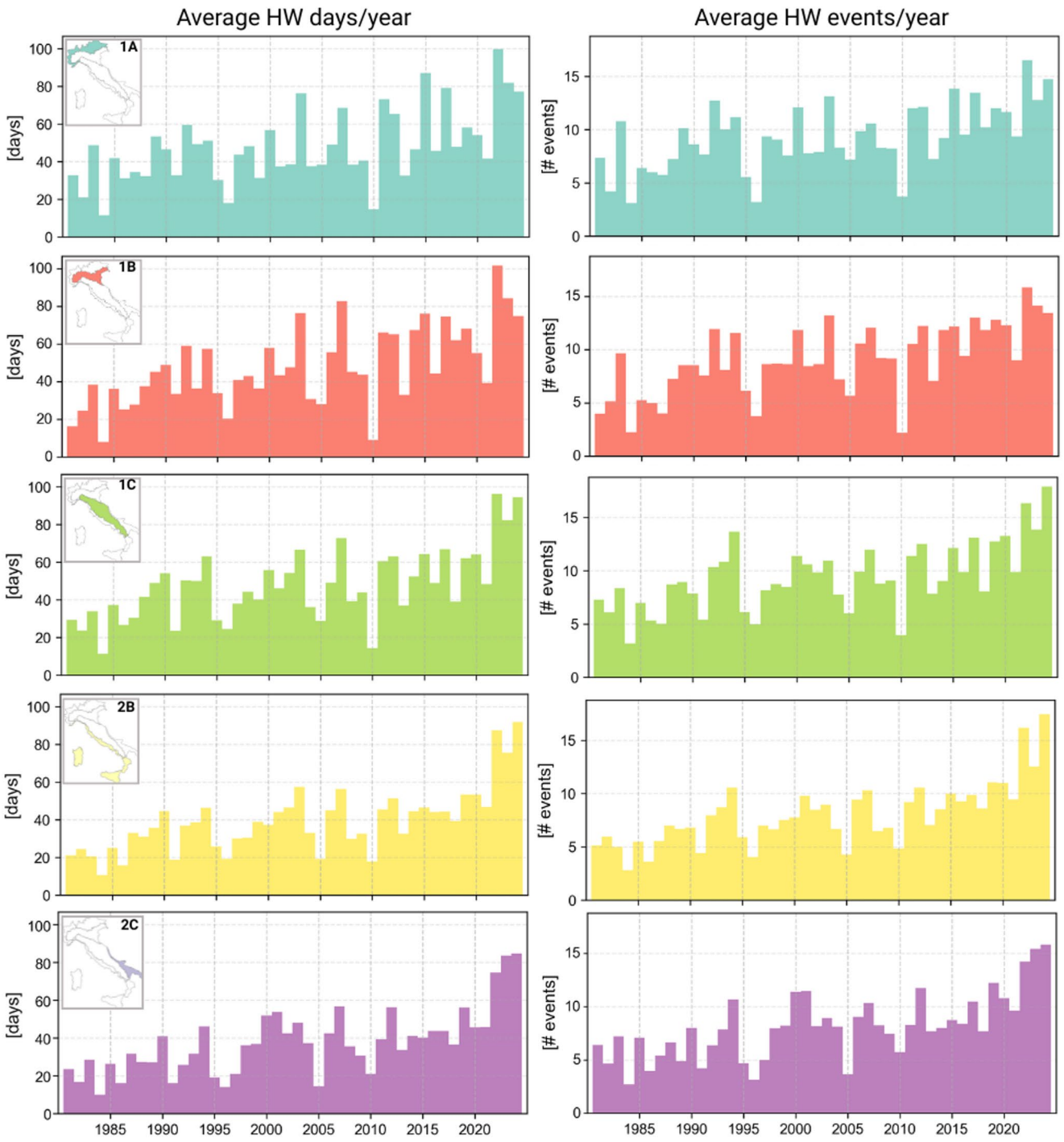

Fig. 11 Average of yearly HW days and HW events in each ecoregion

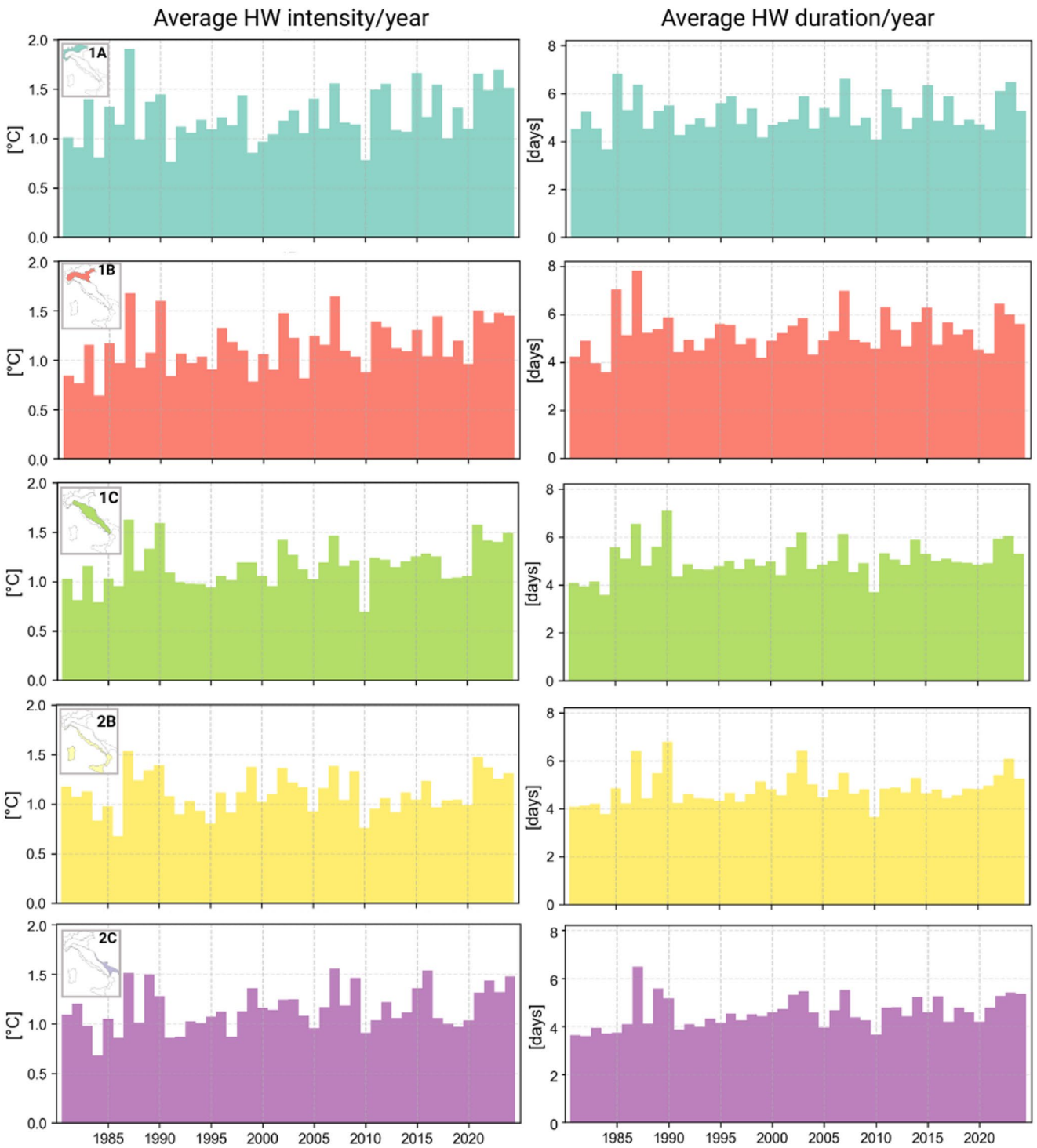

Fig. 12 Average of mean yearly HW intensity and HW duration for each ecoregion

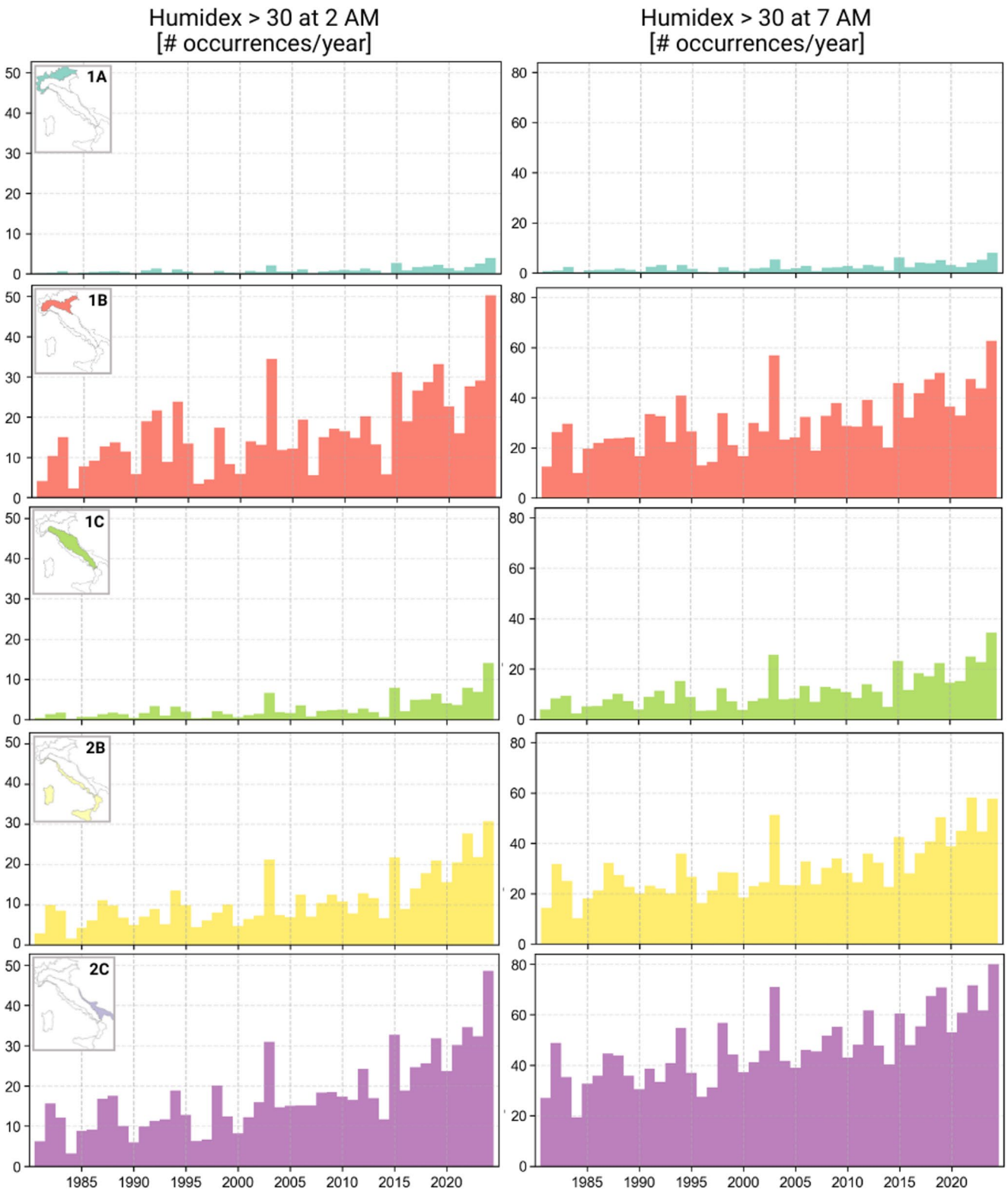

Fig. 13 Average yearly occurrence of Humidex > 30 ("some" discomfort) at 2 AM and 7 AM for each ecoregion. Note that the y-axis scale is different in the left and right panels

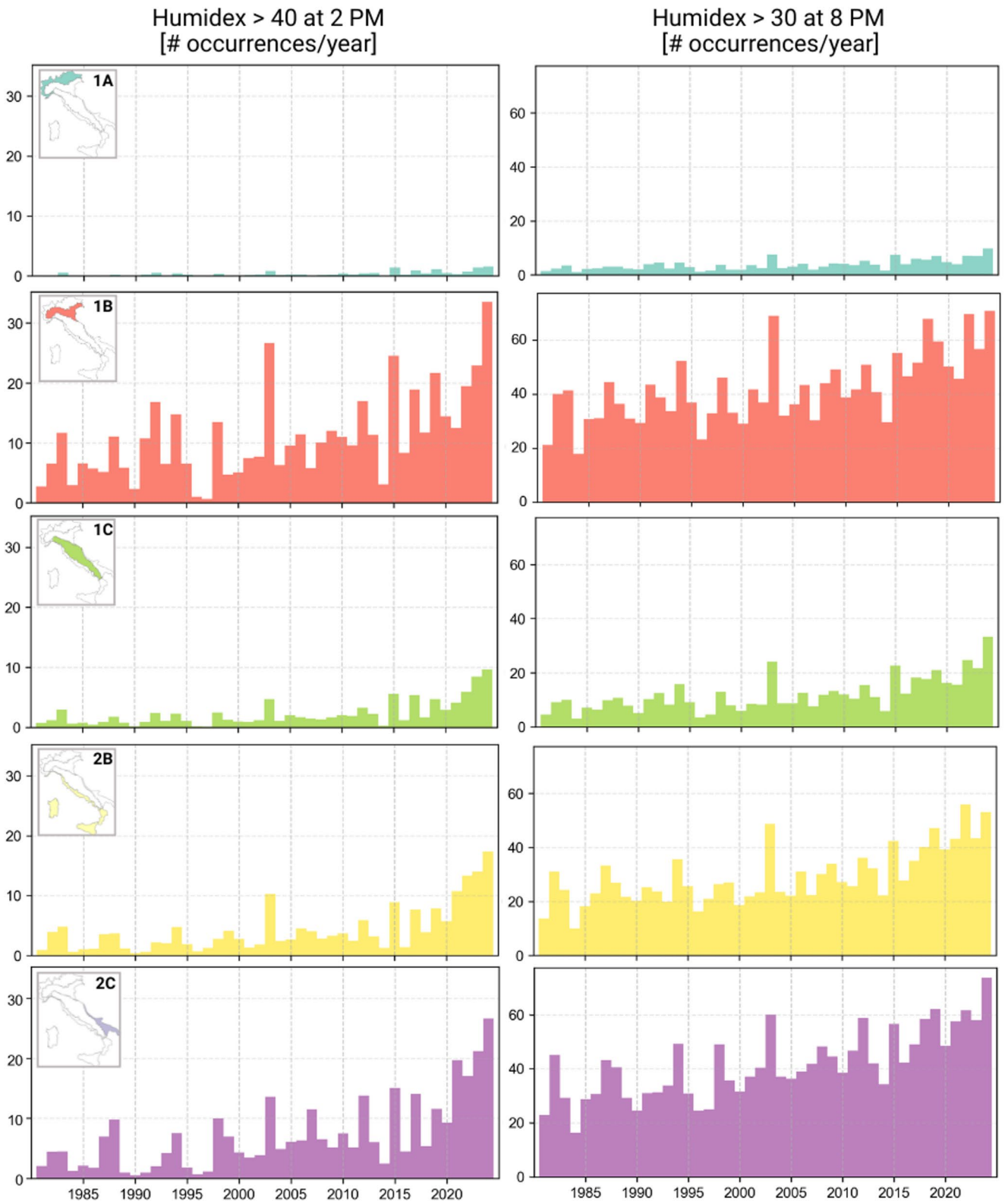

Fig. 14 Average yearly occurrence of Humidex > 40 ("great" discomfort) at 2 PM and Humidex > 30 ("some" discomfort) at 7 AM for each ecoregion. Note that the y-axis scale is different in the left and right panels

Supplementary Information The online version contains supplementary material available at https://doi.org/10.1007/s12518-026-00734-x.

Author contributions Alberto Vavassori (A.V.), Matej Žgela (M.Z.) and Maria Antonia Brovelli (M.A.B.); Methodology: A.V., M.Z. and M.A.B.; Software: A.V. and M.Z.; Formal analysis: A.V. and M.Z.; Investigation: A.V. and M.Z.; Data Curation: A.V. and M.Z.; Visualization: A.V.; Writing - original draft preparation: A.V. and M.Z.; Writing - review and editing: A.V., M.Z. and M.A.B.; Funding acquisition: M.A.B.; Project administration: M.A.B.; Supervision: M.A.B. All authors have read and agreed to the published version of the manuscript.

Funding Open access funding provided by Politecnico di Milano within the CRUI-CARE Agreement. This study was carried out within the Space It Up! project funded by the Italian Space Agency, ASI, and the Ministry of University and Research, MUR, under contract n. 2024-5-E.0 - CUP n. I53D24000060005.

Data availability The VHR-REA_IT reanalysis data is openly available over the CMCC Data Delivery System (https://dds.cmcc.it/, accessed on 8 February 2026). The ground-based station dataset is accessible through the ISPRA SCIA database (https://scia.isprambiente.it/, last access 8 February 2026). The codebase used in this paper is available on GitHub (https://github.com/albertovavassori/Climatic_trends_Italy/tree/main, last access 3 May 2026).

Declarations

Competing interests The authors declare no competing interests.

References

Adinolfi M, Raffa M, Reder A, Mercogliano P (2023) Investigation on potential and limitations of ERA5 reanalysis downscaled on Italy by a convection-permitting model. Clim Dyn 61:4319–4342. https://doi.org/10.1007/s00382-023-06803-w

Ballester J, Quijal-Zamorano M, Méndez Turrubiates RF et al (2023) Heat-related mortality in Europe during the summer of 2022. Nat Med 29:1857–1866. https://doi.org/10.1038/s41591-023-02419-z

Barriopedro D, García-Herrera R, Ordóñez C et al (2023) Heat waves: physical understanding and scientific challenges. Rev Geophys 61:e2022RG000780. https://doi.org/10.1029/2022RG000780

Bartolini G, Di Stefano V, Maracchi G, Orlandini S (2012) Mediterranean warming is especially due to summer season: evidences from Tuscany (central Italy). Theor Appl Climatol 107:279–295. https://doi.org/10.1007/s00704-011-0481-1

Bilgili M, Tokmakci M (2025) Climate change and trends in Europe and globally over the period 1970–2023. Phys Chem Earth Parts A/B/C 139:103928. https://doi.org/10.1016/j.pce.2025.103928

Blasi C, Capotorti G, Copiz R et al (2014) Classification and mapping of the ecoregions of Italy. Plant Biosyst 148:1255–1345. https://doi.org/10.1080/11263504.2014.985756

Boboc L, Dima M, Vaideanu P, Ionita M (2025) Trends and variability of heat waves in Europe and the association with large-scale circulation patterns. Weather Clim Extremes 49:100794. https://doi.org/10.1016/j.wace.2025.100794

Brunet M, Jones PD, Sigró J et al (2007) Temporal and spatial temperature variability and change over Spain during 1850–2005. J Geophys Res Atmos. https://doi.org/10.1029/2006JD008249

Brunetti M, Buffoni L, Mangianti F et al (2004) Temperature, precipitation and extreme events during the last century in Italy. Glob Planet Change 40:141–149. https://doi.org/10.1016/S0921-8181(03)00104-8

Brunetti M, Buffoni L, Maugeri M, Nanni T (2000) Trends of minimum and maximum daily temperatures in Italy from 1865 to 1996. Theor Appl Climatol 66:49–60. https://doi.org/10.1007/s007040070032

Campbell S, Remenyi TA, White CJ, Johnston FH (2018) Heatwave and health impact research: a global review. Health Place 53:210–218. https://doi.org/10.1016/j.healthplace.2018.08.017

Cavalleri F, Viterbo F, Brunetti M et al (2024) Inter-comparison and validation of high-resolution surface air temperature reanalysis fields over Italy. Int J Climatol 44:2681–2700. https://doi.org/10.1002/joc.8475

Croce P, Formichi P, Landi F (2021) Evaluation of current trends of climatic actions in Europe based on observations and regional reanalysis. Remote Sens 13:2025. https://doi.org/10.3390/rs13112025

Curci G, Guijarro JA, Di Antonio L et al (2021) Building a local climate reference dataset: application to the Abruzzo region (Central Italy), 1930–2019. Int J Climatol 41:4414–4436. https://doi.org/10.1002/joc.7081

Díaz-Poso A, Lorenzo N, Royé D (2023) Spatio-temporal evolution of heat waves severity and expansion across the Iberian Peninsula and Balearic Islands. Environ Res 217:114864. https://doi.org/10.1016/j.envres.2022.114864

Desiato F, Fioravanti G, Fraschetti P et al (2011) Climate indicators for Italy: calculation and dissemination. Adv Sci Res 6:147–150. https://doi.org/10.5194/asr-6-147-2011

Domínguez-Castro F, Reig F, Vicente-Serrano SM et al (2020) A multidecadal assessment of climate indices over Europe. Sci Data 7:125. https://doi.org/10.1038/s41597-020-0464-0

Donat MG, Alexander LV, Yang H et al (2013) Updated analyses of temperature and precipitation extreme indices since the beginning of the twentieth century: The HadEX2 dataset. J Geophys Res Atmos 118:2098–2118. https://doi.org/10.1002/jgrd.50150

Durre I, Menne MJ, Gleason BE et al (2010) Comprehensive automated quality assurance of daily surface observations. J Appl Meteorol Climatol 49:1615–1633. https://doi.org/10.1175/2010JAMC2375.1

European Environment Agency (ed) (2024) European climate risk assessment: executive summary. Publications Office of the European Union, Luxembourg

Eurostat (2025) Population structure and ageing. https://ec.europa.eu/eurostat/statistics-explained/index.php?title=Population_structure_and_ageing. Accessed 3 Feb 2026

Fioravanti G, Piervitali E, Desiato F (2016) Recent changes of temperature extremes over Italy: An index-based analysis. Theor Appl Climatol 123:473–486. https://doi.org/10.1007/s00704-014-1362-1

Fratianni S, Acquaotta F (2017) The Climate of Italy. In: Soldati M, Marchetti M (eds) Landscapes and Landforms of Italy. Springer International Publishing, Cham, pp 29–38

Galanaki E, Giannaros C, Kotroni V et al (2022) Spatio-temporal analysis of heatwaves characteristics in Greece from 1950 to 2020. Climate Basel. https://doi.org/10.3390/cli11010005

Giorgi F (2006) Climate change hot-spots. Geophys Res Lett 33:2006GL025734. https://doi.org/10.1029/2006GL025734

Gobiet A, Kotlarski S, Beniston M et al (2014) 21st century climate change in the European Alps—A review. Sci Total Environ 493:1138–1151. https://doi.org/10.1016/j.scitotenv.2013.07.050

Government of Canada CC for OH and S (2025) CCOHS: Humidex Rating and Work. https://www.ccohs.ca/oshanswers/phys_agents/humidex.html. Accessed 26 Jan 2026

Guijarro JA (2018) Homogenization of climatic series with Climatol

Hersbach H, Bell B, Berrisford P et al (2020) The ERA5 global reanalysis. Q J R Meteorol Soc 146:1999–2049. https://doi.org/10.1002/qj.3803

Infusino E, Caloiero T, Fusto F et al (2021) Characterization of the 2017 summer heat waves and their effects on the population of an area of Southern Italy. Int J Environ Res Public Health. https://doi.org/10.3390/ijerph18030970

IPCC (2023) Mediterranean Region. Climate Change 2022 – Impacts, Adaptation and Vulnerability: Working Group II Contribution to the Sixth Assessment Report of the Intergovernmental Panel on Climate Change. Cambridge University Press, Cambridge, pp 2233–72

Klein Tank AMG, Können GP (2003) Trends in indices of daily temperature and precipitation extremes in Europe, 1946–99. J Clim 16:3665–3680. https://doi.org/10.1175/1520-0442(2003)016%253C3665:TIIODT%253E2.0.CO;2

Kohler T, Maselli D (2009) Mountains and climate change: from understanding to action

Kostopoulou E, Jones PD (2005) Assessment of climate extremes in the Eastern Mediterranean. Meteorol Atmos Phys 89:69–85. https://doi.org/10.1007/s00703-005-0122-2

Kottek M, Grieser J, Beck C et al (2006) World map of the Köppen-Geiger climate classification updated. metz 15:259–263. https://doi.org/10.1127/0941-2948/2006/0130

Krähenmann S, Walter A, Brienen S et al (2018) High-resolution grids of hourly meteorological variables for Germany. Theor Appl Climatol 131:899–926. https://doi.org/10.1007/s00704-016-2003-7

Lee J-Y, Marotzke J, Bala G et al (2021) Future global climate. scenario-based projections and near-term information

Manco I, Riviera W, Zanetti A et al (2025) A new conditional generative adversarial neural network approach for statistical downscaling of the ERA5 reanalysis over the Italian Peninsula. Environ Model Softw 188:106427. https://doi.org/10.1016/j.envsoft.2025.106427

Mora C, Dousset B, Caldwell IR et al (2017) Global risk of deadly heat. Nat Clim Change 7:501–506. https://doi.org/10.1038/nclimate3322

Morlot M, Russo S, Feyen L, Formetta G (2023) Trends in heat and cold wave risks for the Italian Trentino-Alto Adige region from 1980 to 2018. Nat Hazards Earth Syst Sci 23:2593–2606. https://doi.org/10.5194/nhess-23-2593-2023

Peña-Angulo D, Reig-Gracia F, Domínguez-Castro F et al (2020) ECTACI: European Climatology and Trend Atlas of Climate Indices (1979–2017). J Geophys Res Atmos 125:e2020JD032798. https://doi.org/10.1029/2020JD032798

Perkins-Kirkpatrick SE, Lewis SC (2020) Increasing trends in regional heatwaves. Nat Commun 11:3357. https://doi.org/10.1038/s41467-020-16970-7

Perkins SE, Alexander LV (2013) On the measurement of heat waves. J Clim 26:4500–4517. https://doi.org/10.1175/JCLI-D-12-00383.1

Peterson TC, Easterling DR, Karl TR et al (1998) Homogeneity adjustments ofin situ atmospheric climate data: a review. Int J Climatol 18(19981115):1493–1517. https://doi.org/10.1002/(SICI)1097-0088(19981115)18:13%253C1493::AID-JOC329%253E3.0.CO;2-T

Prete G, Avolio E, Capparelli V et al (2023) Daily precipitation and temperature extremes in Southern Italy (Calabria Region). Atmosphere 14:553. https://doi.org/10.3390/atmos14030553

Rachid A, Qureshi AM (2023) Sensitivity analysis of heat stress indices. Climate 11:181. https://doi.org/10.3390/cli11090181

Raffa M, Reder A, Marras GF et al (2021) VHR-REA_IT Dataset: Very High Resolution Dynamical Downscaling of ERA5 Reanalysis over Italy by COSMO-CLM. Data 6:88. https://doi.org/10.3390/data6080088

Rockel B, Will A, Hense A (2008) The regional climate model COSMO-CLM (CCLM). Meteorol Z 17:347–348. https://doi.org/10.1127/0941-2948/2008/0309

Russo S, Sillmann J, Fischer EM (2015) Top ten European heatwaves since 1950 and their occurrence in the coming decades. Environ Res Lett 10:124003. https://doi.org/10.1088/1748-9326/10/12/124003

Sajjad H, Ghaffar A (2019) Observed, simulated and projected extreme climate indices over Pakistan in changing climate. Theor Appl Climatol 137:255–281. https://doi.org/10.1007/s00704-018-2573-7

Schwingshackl C, Sillmann J, Vicedo-Cabrera AM et al (2021) Heat stress indicators in CMIP6: estimating future trends and exceedances of impact-relevant thresholds. Earths Future 9:e2020EF001885. https://doi.org/10.1029/2020EF001885

Scoccimarro E, Fogli PG, Gualdi S (2017) The role of humidity in determining scenarios of perceived temperature extremes in Europe. Environ Res Lett 12:114029. https://doi.org/10.1088/1748-9326/aa8cdd

Scorzini AR, Leopardi M (2019) Precipitation and temperature trends over central Italy (Abruzzo Region): 1951–2012. Theor Appl Climatol 135:959–977. https://doi.org/10.1007/s00704-018-2427-3

Settanta G, Fraschetti P, Lena F et al (2024) Recent tendencies of extreme heat events in Italy. Theor Appl Climatol 155:7335–7348. https://doi.org/10.1007/s00704-024-05063-w

Simmons AJ, Berrisford P, Dee DP et al (2017) A reassessment of temperature variations and trends from global reanalyses and monthly surface climatological datasets. Q J R Meteorol Soc 143:101–119. https://doi.org/10.1002/qj.2949

Simolo C, Brunetti M, Maugeri M, Nanni T (2014) Increasingly warm summers in the Euro–Mediterranean zone: mean temperatures and extremes. Reg Environ Change 14:1825–1832. https://doi.org/10.1007/s10113-012-0373-7

Sirangelo B, Caloiero T, Coscarelli R et al (2020) Combining stochastic models of air temperature and vapour pressure for the analysis of the bioclimatic comfort through the Humidex. Sci Rep 10:11395. https://doi.org/10.1038/s41598-020-68297-4

Terando A, Easterling WE, Keller K, Easterling DR (2012) Observed and modeled twentieth-century spatial and temporal patterns of selected agro-climate indices in North America. J Clim 25:473–490. https://doi.org/10.1175/2011JCLI4168.1

Toreti A, Desiato F (2008) Temperature trend over Italy from 1961 to 2004. Theor Appl Climatol 91:51–58. https://doi.org/10.1007/s00704-006-0289-6

Turco M, Zollo AL, Ronchi C et al (2013) Assessing gridded observations for daily precipitation extremes in the Alps with a focus on Northwest Italy. Nat Hazards Earth Syst Sci 13:1457–1468. https://doi.org/10.5194/nhess-13-1457-2013

United Nations, Department of Economic and Social Affairs, Population Division (2024) (2024) World Population Prospects 2024. https://population.un.org/dataportal/home?df=c40473c9-4cb1-45b4-adc5-4571c16a0eb8. Accessed 9 Feb 2026

WMO (2024) Guide to Instruments and Methods of Observation (WMO-No. 8), Volume I – Measurement of Meteorological Variables. World Meteorological Organization (WMO). https://library.wmo.int/idurl/4/68695. Accessed 9 Feb 2026

Yasmeen S, Liu H (2019) Evaluation of thermal comfort and heat stress indices in different countries and regions – A Review. IOP Conf Ser: Mater Sci Eng 609:052037. https://doi.org/10.1088/1757-899X/609/5/052037

Yavaşlı DD (2025) Thermal persistence index (TPI): A novel measure of prolonged heat stress in the Mediterranean, 1950–2024. Theor Appl Climatol 157:28. https://doi.org/10.1007/s00704-025-05972-4

Zwiers FW, Zhang X (2009) Guidelines on Analysis of extremes in a changing climate in support of informed decisions for adaptation. https://library.wmo.int/idurl/4/48826. Accessed 9 Feb 2026